

RESEARCH PAPER



Mitochondrial dysfunction generates a growth-restraining signal linked to pyruvate in *Drosophila* larvae

Jack George ^a, Tea Tuomela ^a, Esko Kemppainen ^a, Antti Nurminen^a, Samuel Braun^a, Cagri Yalgin^{a,b}, and Howard T. Jacobs^{a,b}

^aFaculty of Medicine and Health Technology, Tampere University, Tampere, Finland; ^bInstitute of Biotechnology, University of Helsinki, Helsinki, Finland

ABSTRACT

The *Drosophila* bang-sensitive mutant *tko*^{25t}, manifesting a global deficiency in oxidative phosphorylation due to a mitochondrial protein synthesis defect, exhibits a pronounced delay in larval development. We previously identified a number of metabolic abnormalities in *tko*^{25t} larvae, including elevated pyruvate and lactate, and found the larval gut to be a crucial tissue for the regulation of larval growth in the mutant. Here we established that expression of wild-type *tko* in any of several other tissues of *tko*^{25t} also partially alleviates developmental delay. The effects appeared to be additive, whilst knock-down of *tko* in a variety of specific tissues phenocopied *tko*^{25t}, producing developmental delay and bang-sensitivity. These findings imply the existence of a systemic signal regulating growth in response to mitochondrial dysfunction. Drugs and RNAi-targeted on pyruvate metabolism interacted with *tko*^{25t} in ways that implicated pyruvate or one of its metabolic derivatives in playing a central role in generating such a signal. RNA-seq revealed that dietary pyruvate-induced changes in transcript representation were mostly non-coherent with those produced by *tko*^{25t} or high-sugar, consistent with the idea that growth regulation operates primarily at the translational and/or metabolic level.

ARTICLE HISTORY

Received 7 May 2019
Revised 26 August 2019
Accepted 28 August 2019
Published online 13
September 2019

KEYWORDS

Mitochondria; protein synthesis; lactic acidosis; respiration; translation; larva



Introduction


Mitochondrial dysfunction is a common underlying cause or manifestation of human disease [1–3]. Whilst mammalian models such as the mouse have provided insights into the underlying processes, the use of *Drosophila* to understand mitochondrial pathophysiology has been relatively neglected, despite its versatility and the availability of a wide variety of easily applied genetic tools.

Deficient mitochondrial protein synthesis is frequently associated with mitochondrial diseases [4], and *Drosophila* provides a valuable model to study the physiological effects of limitations on mitochondrial translation in the context of animal development. The *Drosophila tko* gene, encoding mitoribosomal protein S12, a core component of the mitoribosomal decoding centre, has been a particular object of study in this regard. The canonical mutant *tko*^{25t} displays a range of phenotypic features that resemble mitochondrial disease in humans, including developmental delay, impaired sound-responsiveness, bang-

sensitivity (paralytic seizures induced by mechanical shock) and antibiotic sensitivity [5]. Other *tko*^{25t} phenotypes are unique to *Drosophila*, such as male courtship defect [5]. These phenotypic features reflect an underlying deficiency of mitoribosomes [5] and consequent global deficiency of the enzymatic functions of oxidative phosphorylation (OXPHOS) that depend upon mitochondrial translation products, manifesting in both adults [5] and larvae [6]. All of these phenotypes are reversed by ubiquitous expression of a transgenic copy of the wild-type *tko* gene, using the UAS/GAL4 system [6]. Since developmental delay occurs during the larval stages [5], this prompts the question as to which of the larval tissues mediates the crucial signalling that regulates growth in response to limitations on mitochondrial protein synthesis, and by what mechanism.

In a follow-up study [7], we obtained some relevant clues as to the underlying mechanism(s) whereby the growth rate of *tko*^{25t} larvae is adjusted, so as to take account of the decreased capacity for processing

CONTACT Howard T. Jacobs  howard.jacobs@tuni.fi  Faculty of Medicine and Health Technology, FI-33014 Tampere University, Tampere FI-33014, Finland

 Supplemental data for this article can be accessed [here](#).

© 2019 The Author(s). Published by Informa UK Limited, trading as Taylor & Francis Group. This is an Open Access article distributed under the terms of the Creative Commons Attribution-NonCommercial-NoDerivatives License (<http://creativecommons.org/licenses/by-nc-nd/4.0/>), which permits non-commercial re-use, distribution, and reproduction in any medium, provided the original work is properly cited, and is not altered, transformed, or built upon in any way.

nutritional resources caused by mitochondrial dysfunction. In particular, we observed that components of the apparatus of cytosolic protein synthesis and secretion were down-regulated in *tko*^{25t} larvae, both at the transcript level and via a key regulatory step of cytosolic protein synthesis, the ribosomal protein S6 kinase (S6K). *tko*^{25t} larvae were also found to be unaffected by low levels of the cytosolic protein synthesis inhibitor cycloheximide, which retarded the development of wild-type larvae, also implicating the cytoribosome as a crucial target in larval growth regulation. Many other genes that were downregulated in *tko*^{25t} at the RNA level encoded secreted proteins of the gut and cuticle, suggesting that growth rate in *tko*^{25t} could be adjusted to compensate for stress in the protein secretory system caused by disruption of redox homeostasis.

In the same study [7] we determined that the strength of the *tko*^{25t} phenotype depends upon the culture conditions, specifically the sugar content of the growth medium. When *tko*^{25t} flies were cultured on high-sugar medium, their growth was further impaired compared with those grown on low-sugar medium, and many of the observed changes in gene expression were more pronounced. The effect of high sugar was accompanied by increases in the level of pyruvate and lactate in the larvae, whilst supplementation of the medium with pyruvate or lactate exacerbated developmental delay. *tko*^{25t} larvae also manifested low levels of ATP and a greatly decreased NADPH/NADP ratio, both of which were enhanced by high-sugar medium [7].

A key result from the previous study was the observation that expression of wild-type *tko* specifically in portions of the larval gut, a major secretory tissue, partially alleviated the developmental delay of *tko*^{25t} [7]. Since the driver used in this experiment did not express at a high level in all regions of the gut, we reasoned that other gut-specific drivers used in combination might provide a more complete rescue of the phenotype. To embark on such a study, we initially implemented what we assumed would be negative controls, directing wild-type *tko* expression in other regions of the larva with high specificity. However, this produced the unexpected result that partial rescue of developmental delay was conferred by expression in each of the tissues tested (muscle, fat-body, neurons, as well as gut), with some evidence of additive effects. Conversely, *tko* knockdown in each specific

tissue produced a partial developmental delay, accompanied by bang sensitivity, the canonical adult phenotype of *tko*^{25t}.

These new findings indicate the existence of a systemic and possibly metabolic signal integrating growth across the entire larva, in response to limitations on mitochondrial translational or OXPHOS capacity. Given the previous findings implicating pyruvate and/or lactate as key regulatory metabolites, we studied the effects of drugs and RNAi targeted on pyruvate and its metabolic transactions. The findings are consistent with pyruvate metabolism playing a central role in generating the signal that links growth and mitochondrial function in *Drosophila* larvae.

Materials and methods

Drosophila strains and culture

Drosophila strains were procured from stock centres, supplied by colleagues or maintained long term in our laboratory. A full list of GAL4 drivers, RNAi lines and other strains used in the study are provided in Tables 1, 2 and 3, respectively. Markers carried on standard balancers were used to distinguish experimental from control progeny. Except where stated, flies were cultured on standard high-sugar medium (HS), as detailed in [7]. A variant, ‘zero-sugar’ medium (ZS), containing standard dietary supplements but no added sugars [7], was used where indicated. Note that HS and ZS media are not isocaloric: in an earlier study [7] the extent of developmental delay in *tko*^{25t} flies was shown to depend only on the sugar content of the medium, not its calorific value. Sodium pyruvate, dichloroacetate or UK5099 (Sigma-Aldrich), were added to these media from aqueous stock solutions after the medium had been cooled to below 65°C, giving the final concentrations indicated in the figures.

Developmental and bang-sensitivity assays

Mean developmental time to eclosion and bang-sensitivity were measured as previously [5,7], in temperature-controlled incubators, with temperature verified daily throughout the experiment. In all crosses where developmental time to eclosion was measured, at least 3 (usually 4) replicate vials were studied, and the entire experiment was repeated to validate the findings.

Table 1. GAL4 drivers used in the study.

Name ^a	Stock centre ID ^b or source	Alias, if any	Chromosome	Expression pattern ^c	References ^d
<i>da</i> -GAL4	BL 8641		3	ubiquitous	[8]
<i>gut</i> -GAL4	KY 113094	NP3084	2	midgut, proventriculus, gastric ceca, salivary glands	[7,9], Fig. S1
<i>elav</i> -GAL4	BL 458	c155	X	neurons, embryonic neuroblasts and glioblasts	[10,11]
<i>nrv2</i> -GAL4	BL 6800		2	glial cells, weak expression in some neurons	[12–16], Fig. S1
G14	kind gift of John Sparrow	G14-Gal4	2	muscle, salivary glands	[17–19]
<i>Mef2</i> -GAL4	BL 27390	GAL4-Mef2, DMef2-GAL4	3	muscle	[20]
<i>Kr</i> -GAL4	kind gift of John Sparrow		2	early embryo, larval midgut	[21,22], Fig. S1
<i>Lsp2</i> -GAL4	BL 6357		3	Fat body (third larval instar and adult)	[23,24], Fig. S1

^aas used here.

^bBL = Bloomington, KY = Kyoto.

^cconsensus or most recent revision from published literature, or based on figures of this paper.

^dliterature citation(s) or figure of this paper.

Table 2. RNAi lines used in the study.

Symbol of targeted gene	Stock centre ID ^a	Library	Chromosome (insertion)	Reference ^b
<i>tko</i>	BL 38251	TRiP	2	[25,26]
<i>Mpc1</i>	BL 67817	TRiP	2	[25,27]
<i>Pdk</i>	BL 28635	TRiP	3	[25,26]
<i>Men</i>	BL 38256	TRiP	2	[25,26]
<i>Men</i>	VDRC 330428	shRNA	2	[28]
<i>Men</i>	VDRC 104016	KK	2	[28,29]
<i>Men-b</i>	BL 57489	TRiP	2	[25,27]
<i>Men-b</i>	VDRC 100812	KK	2	[28,29]
<i>Ldh</i>	VDRC 110190	KK	2	[29]

^aBL = Bloomington, VDRC = Vienna Drosophila Research Centre.

^bliterature citation(s).

RNA analysis

Quantitative reverse-transcription PCR (qRT-PCR) to confirm the effectiveness of RNAi was conducted as previously [7,37], using RpL32 as an

internal standard and verified primer pairs (all shown 5' to 3') as follows: for *Pdk* – GGATTCG GAACAGATGCAAT and CGCGATAGAACTTT GAGCTTG, for *Mpc1* – GCCGACACACAAA AGAGTCC and GCTGGACCTTGTAGGCAAAT, for *Men* – ACTCGATCCTACGACGCTGT and TGAGGAAGGACTCTGCGAAT. RNA sequencing and data analysis were carried out as previously [7], using RNA from Oregon R or *tko*^{25t} L3-stage larvae cultured on different media. Note that initial statistical filtering by Cuffdiff (chipster.csc.fi) excludes genes in any pairwise comparison where the differences fail significance testing, regardless of their magnitude. For further analysis (see Results), arbitrary thresholds were then applied to restrict the analysis to genes showing substantial differences in expression, as measured by either of two parameters: >8 fold change

Table 3. Other *Drosophila* strains used in the study.

Name ^a	Stock centre ID ^b	Alias, if any	Chromosome (insertion, mutation or balancer)	Other features ^c	References ^d
<i>tko</i> ^{25t}	n/a	<i>tko</i> (25t)	X	Bang-sensitive; coding-region mis-sense mutant	[30–32]
UAS- <i>tko</i> ⁺ (1)	n/a		3	transgenic for wild-type copy of <i>tko</i> cDNA; without driver does not alleviate bang sensitivity of <i>tko</i> ^{25t}	[6]
UAS- <i>tko</i> ⁺ (8)	n/a		2	transgenic for wild-type copy of <i>tko</i> cDNA; without driver does not alleviate developmental delay of <i>tko</i> ^{25t}	[6]
FM7	BL 995		X	balancer chromosome	[33]
CyO	BL 4959		2	balancer chromosome	[34]
TM3Sb	n/a	TM3-Sb	3	balancer chromosome, currently available from stock centre combined with CyO	[34]
UAS-Stinger	BL 65402	UAS-GFP, UAS-Stinger	2	transgenic expressor of nuclear-targeted GFP	[35]
UAS-mCD8-GFP	KY 108068	mCD8-GFP, + many variants	2	transgenic expressor of membrane-targeted GFP	[36]

^aas used here.

^bBL = Bloomington, KY = Kyoto, n/a not currently available from stock centres.

^cconsensus or most recent revision from published literature, or based on figures of this paper.

^dliterature citation(s) or figure of this paper (Figure 1).

or >100 units of FPKM (mass fraction). Raw sequence data have been deposited at ArrayExpress (www.ebi.ac.uk/ArrayExpress/).

Metabolite analysis

Batches of 20 larvae were homogenized in 100 μ l of 6M guanidine hydrochloride on ice. The homogenate was incubated at 95°C for 5 min and centrifuged at 12000g_{max} for 5 min at 4°C. The supernatants were stored at -80°C, and later diluted 1:10 and with PBS (pH 7.4) for analysis. Pyruvate and lactate were measured with commercially available fluorescence-based determination kits (Abcam) according to manufacturer's instructions. 10 μ l of sample was combined with 50 μ l of either lactate or pyruvate reaction mix, incubated at room temperature for 30 min after which fluorescence was measured (excitation at 535 nm, emission at 590 nm) using a plate reader. Lactate and pyruvate standards were used to generate standard curves and concentrations were normalized to soluble protein as measured using the Bradford method.

Statistics

For pairwise comparisons between groups, the two-tailed (unpaired) Student's *t* test (Microsoft Excel) was applied. For multiple comparisons, we used one-way ANOVA with Tukey *post hoc* HSD test online (astatsa.com). For comparisons where multiple factors were being assessed, two-way ANOVA (GraphPad Prism or online tool at vassartstats.net/anova2u.html, as indicated) was used, together with Dunnett's or Tukey's *post hoc* multiple comparisons tests as indicated, where interactions were detected, or where more than two levels were compared.

Results

Wild-type *tko* expression in diverse tissues alleviates developmental delay in *tko*^{25t}

Using the line UAS-*tko*⁺(8) [6], in which a wild-type *tko* transgene is expressed under the control of GAL4, we tested the tissue-specificity of developmental delay in the *tko*^{25t} background, by combining it with different GAL4 drivers directing distinct tissue patterns of expression. In addition to almost complete rescue

using *da*-GAL4 and the partial rescue with gut-GAL4 documented previously, we found that drivers specific for the fat body (*Lsp2*-GAL4), muscle (G14 and *Mef2*-GAL4) and CNS (neurons, *elav*-GAL4) all gave a partial rescue (Figure 1), although this was most pronounced or significant in each case at different characteristic temperatures (Table S1).

We confirmed the specificity of patterns of expression of these drivers using GAL4-dependent constructs for GFP (Fig. S1). The alleviation of the phenotype was due to a positive effect of the transgene/driver combination, and not due to a negative effect of the CyO balancer chromosome in the *tko*^{25t} background (Fig. S2). Note, however, that this was not true of the TM3Sb balancer (Fig. S2), the use of which was therefore avoided in all experiments described.

The partial rescue produced by several drivers appeared to be additive, based on two lines of evidence. First, we attempted to combine pairs of drivers and the UAS-*tko*⁺(8) transgene. This experiment was technically challenging for several reasons: the problematic nature of the TM3Sb balancer precluded its use; some transgenic combinations had poor viability, especially as homozygotes, and the drivers did not all perform optimally at the same temperature. However, the combination of the fat-body and muscle drivers *Lsp2*-GAL4 and G14 appeared to give an additive enhancement at 22°C (Fig. S3), although this should be interpreted cautiously, due to the imperfect experimental design. The second piece of evidence for a combinatorial effect was that a second transgenic line, UAS-*tko*⁺(1), which already showed a one-day alleviation of developmental delay compared with *tko*^{25t} flies bearing no transgene [6], showed a further alleviation of developmental delay when combined with different GAL4 drivers (Figure 2). These findings suggest the operation of a systemic signal that integrates the degree of mitochondrial dysfunction across tissues, calibrating growth to the ability of the organism to process nutritional resources.

RNAi-mediated *tko* knockdown in diverse tissues phenocopies *tko*^{25t}

To further test this hypothesis, we used RNA-mediated knockdown of *tko* to profile the tissues in which the resulting mitochondrial translational deficit leads to a *tko*^{25t}-like phenotype. Ubiquitous *tko* knockdown using the *da*-GAL4 driver and the

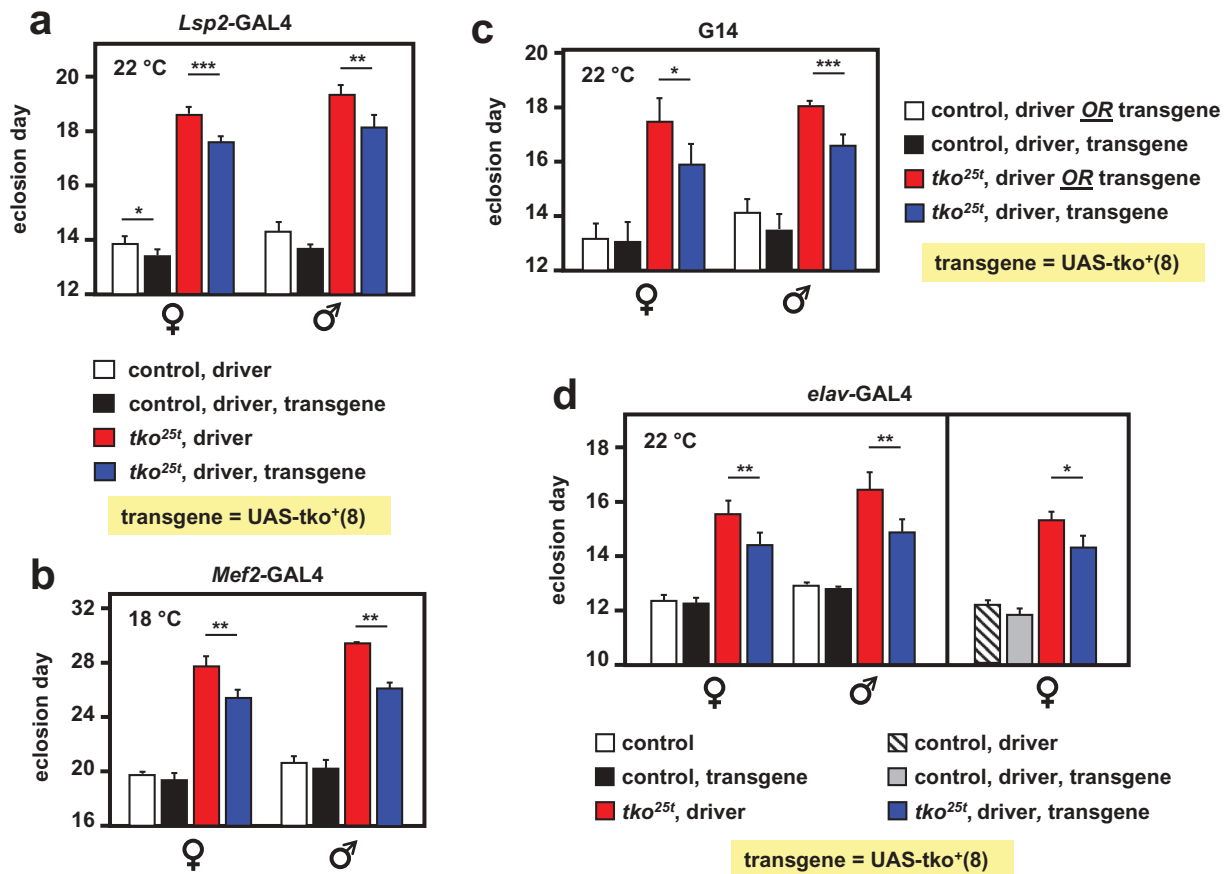


Figure 1. *tko*^{25t} developmental delay is partially alleviated by *tko*⁺ expression directed by different drivers. Time to eclosion (means \pm SD, $n \geq 3$ replicate vials for each cross), of flies of the indicated genotypes, using UAS-*tko*⁺(8) with the indicated drivers. Controls were FM7 balancer flies with (a, b and d – right-hand panel) driver but no transgene, (c), driver *or* transgene (these classes could not be distinguished due to the nature of the cross, since the G14 driver is not viable as a homozygote), and (d – left-hand panel) neither transgene nor driver, as dictated by the chromosomal location of the drivers. Because the *elav*-GAL4 driver is located on the X chromosome, one of the two reciprocal crosses used in (d) generates only informative females and not males. Horizontal lines denoted by asterisks (*, **, ***) indicate significant differences in pairwise comparisons of flies of a given sex and *tko* genotype, with and without actively driven *tko*⁺ (Student's *t* test, $p < 0.05$, 0.01, 0.001, respectively). The specificity of each driver was confirmed by parallel crosses in which it was used to direct the synthesis of nuclear- or membrane-localized GFP (see Fig. S1). Note that we avoided the use of the TM3 balancer because we established that it conferred a developmental delay in conjunction with *tko*^{25t}, whereas the chromosome 2 balancer CyO did not (Fig. S2). The partial rescue of developmental delay was also observed at other temperatures with some drivers (see Table S1) and using the alternate transgene UAS-*tko*⁺(1) – see Figure 2. Note that most GAL4 drivers exhibit the classic pattern of temperature dependence [38], i.e. increased activity at higher temperature. However, for the strongest drivers, this may also lead to deleterious effects of over-expression at high temperature, such that a lower temperature produces optimal effects.

Bloomington TRiP line 38251 targeted on *tko* resulted in a phenotype resembling an exaggerated version of *tko*^{25t}. At 25°C *tko* knockdown was lethal, whilst at 22°C, it was lethal to males and semilethal to females, which eclosed with a long delay (5–9 d) and were too weak to permit a meaningful test of their bang-sensitivity. At 18°C females eclosed with a 7 to 8-d delay (Figure 3(a)) and were highly bang-sensitive (Figure 4(a)), whilst the few males that eclosed were even more delayed (Figure 3(a)) and extremely weak. Knockdown

using tissue-specific drivers produced a milder version of the same phenotype, whether knockdown was targeted specifically to neurons (using *elav*-GAL4, Figures 3(b), 4(b)) or muscle (*Mef2*-GAL4 at 18°C, Figures 3(c), 4(c)). Even more limited knockdown targeted on the early embryo, and portions of the midgut (*Kr*-GAL4, Figure 3(d), Fig. S1) also produced a significant, though very modest developmental delay, but without bang-sensitivity (Figure 4(e)). *Mef2*-GAL4-driven *tko* knockdown at higher temperatures (22, 25°C) again gave

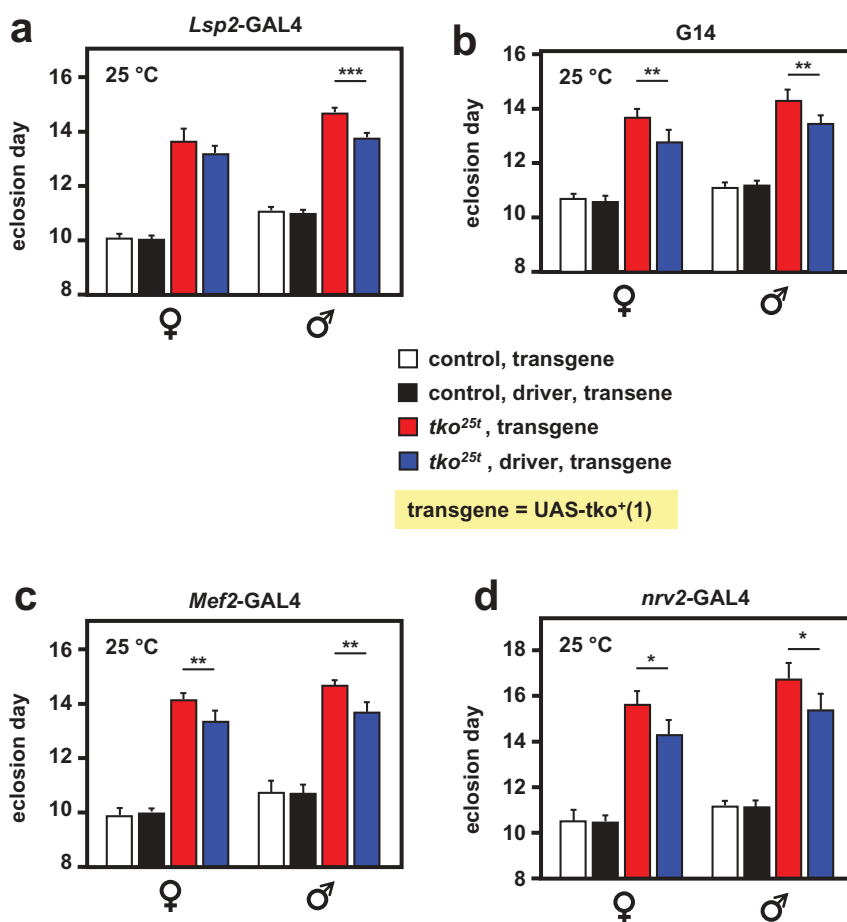


Figure 2. Alleviation of *tko*^{25t} developmental delay in a second UAS-*tko*⁺ line. Time to eclosion at 25°C (means ± SD, n ≥ 3 replicate vials for each cross), of flies of the indicated genotypes, using various drivers plus the UAS-*tko*⁺(1) transgene, shown previously to confer a modest rescue of developmental delay without any driver [6]. Controls were FM7 balancer flies with transgene but without driver, as shown. Horizontal lines denoted by asterisks (*, **, ***) indicated significant differences in pairwise comparisons of flies of a given sex and *tko* genotype, with and without actively driven *tko*⁺ (Student's *t* test, *p* < 0.05, 0.01, 0.001, respectively). The specificity of each driver was confirmed by parallel crosses in which it was used to direct the synthesis of nuclear- or membrane-localized GFP (see Figure S1). Note that we avoided the use of the TM3 balancer because we established that it conferred a developmental delay in conjunction with *tko*^{25t}, whereas the chromosome 2 balancer CyO did not (Fig. S2).

semilethality and severe weakness, which was more severe in males. *elav-GAL4*-driven knockdown also gave sex- and temperature-dependent bang-sensitivity: at 25°C flies were extremely weak, whilst developmental delay was seen at all temperatures but was generally significant only in males (Figure 4(b)). Driving *tko* knockdown with the glial driver *nrv2-GAL4* gave no bang sensitivity (Figure 4(d)).

Drugs that affect pyruvate metabolism impact larval growth

In principle, a systemic signal regulating growth according to mitochondrial function could be endocrine or metabolic in nature. Candidate metabolites

for such a role that were previously shown to be markedly abnormal in *tko*^{25t} larvae, include pyruvate and lactate, which were approximately threefold elevated, and NADPH and ATP, which were highly depleted [7]. Since ATP and NADPH may be considered too labile to perform an intercellular role, we focused our attention on pyruvate and lactate, which are interconvertible through lactate dehydrogenase, and which were previously found to exacerbate and phenocopy the developmental delay of *tko*^{25t}, when added to the medium ([7], Figure 5(a)). We investigated the developmental effect of two drugs known to affect pyruvate metabolism, dichloroacetate (DCA), an inhibitor of pyruvate dehydrogenase kinase (Pdk) and UK5099, an inhibitor of the mitochondrial pyruvate carrier, which could be predicted to have

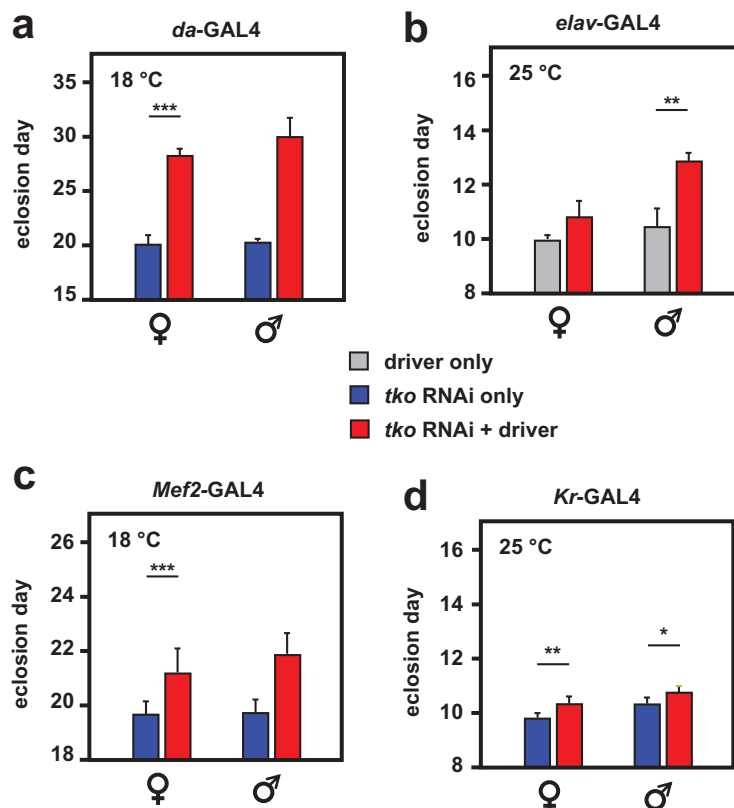


Figure 3. RNAi knockdown of *tko* by different drivers results in developmental delay. Times to eclosion (means \pm SD, $n \geq 3$ replicate vials for each cross) for flies of the indicated sex and genotype, using the various drivers at the temperatures shown. Horizontal lines denoted by asterisks (*, **, ***) indicate significant differences in pairwise comparisons between knockdown and control flies of a given sex, using a given driver (Student's *t* test, $p < 0.05$, 0.01 , 0.001 , respectively). Note that males were in general more severely affected and in some cases (e.g. *da-GAL4*) too few males eclosed to permit a statistically meaningful analysis. Note that most GAL4 drivers exhibit the classic pattern of temperature dependence [38], i.e. increased activity at higher temperature. However, for the strongest drivers this may also lead to highly deleterious effects at high temperature, such that, at a lower temperature, results are more informative.

opposite effects on mitochondrial pyruvate utilization. We tested different concentrations of pyruvate and DCA for their effects on the development of wild-type and *tko*^{25t} females in ZS medium (Figure 5(b)), and performed a more extensive study at single, effective concentrations on different media and both sexes, including heterozygous *tko*^{25t} females (Figure 5(a)). Like pyruvate, DCA produced an additional, dose-dependent developmental delay in both *tko*^{25t} as well as in wild-type flies (Figure 5(a, b, S5)).

UK5099 (25 μ g/ml) also exacerbated the developmental delay of *tko*^{25t}, but had no significant effect on the eclosion timing of wild-type flies (Figure 5(a, S5)).

Genetic manipulations that affect pyruvate metabolism impact larval growth and survival

Next, we analyzed the effects of knocking down the genes coding for the key proteins of pyruvate

metabolism targeted by these drugs. The mitochondrial pyruvate carrier is a heterodimer of the ubiquitous subunit Mpc1 (CG14290) and a differentially expressed second subunit, Mpc2, encoded in *Drosophila* by a small gene family (CG9396, CG9399 and CG32832, the latter being testis specific). Pdk is encoded by a single-copy gene (*Pdk*, CG8808). Using the available RNAi lines for *Mpc1* and *Pdk* from the Harvard Medical School TRiP library, we first confirmed that knockdown for each of the two genes using the ubiquitously acting *daGAL4* driver gave viable flies, and used qRT-PCR to verify that knockdown was effective at the RNA level (Figure 6(a)). We then evaluated the effects of knockdown on wild-type and *tko*^{25t} flies grown in standard high-sugar medium, or on medium supplemented with 25 mg/ml pyruvate (Figure 6(b)). *Mpc1* or *Pdk* knockdown produced no effect on eclosion timing in wild-type flies cultured on standard medium. However, when pyruvate was

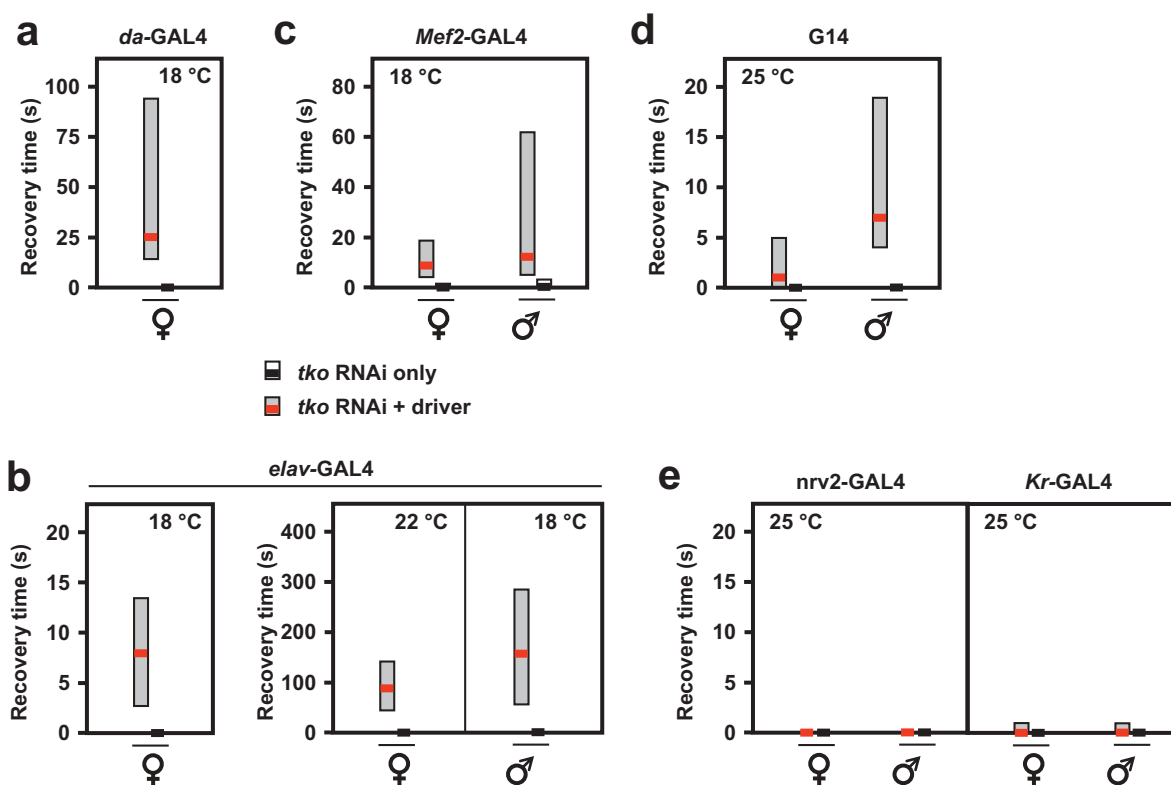


Figure 4. RNAi knockdown of *tko* by different drivers results in bang-sensitivity. Box-plots of recovery times from mechanical shock (bold black or red lines – medians, respectively, for controls and *tko* knockdown flies, with filled boxes representing first to third quartiles) of flies of the indicated genotype, sex and culture temperature. Note the different scales required to plot these data. White bars for control flies were in most cases not plottable, since median and both quartiles were at or very close to zero.

added to the medium, *Mpc1* knockdown exacerbated the developmental delay produced in wild-type flies, but not that of *tko*^{25t} (Figure 6(b), panel i), whilst *Pdk* knockdown had no effect on eclosion timing of wild-type flies on either medium, but mildly alleviated the developmental delay of *tko*^{25t} (Figure 6(b), panel ii) on pyruvate-supplemented medium (see Fig. S6 for summary of the relevant statistical analyses by two-way ANOVA).

Knockdown of two other genes of pyruvate metabolism, coding, respectively, for the cytosolic and mitochondrial isoforms of malic enzyme, produced more dramatic results in combination with *tko*^{25t}. In our previous study, we observed that knockdown of *Men*, the gene encoding the cytosolic isoenzyme, produced no significant effects on *tko*^{25t} (Figure 4(c) of [7]). In the present study we were able to make use of more potent and specific TRiP lines for *Men*, as well as one further dsRNA line from the VDRC collection, all of which gave a strong knockdown of the gene at the RNA level under the control of *da-GAL4* (Figure 7(a)), but had no significant effect

on the development of otherwise wild-type flies (Figure 7(b)). However, in combination with *tko*^{25t} they were all developmentally lethal or semilethal at both 29°C and 25°C (Figure 7(c)). Both of the *Men-b* knockdown lines produced a developmental delay in wild-type flies, and were again synthetically lethal with *tko*^{25t} (Fig. S4), but this result should be interpreted cautiously, since we were not able to demonstrate convincing and consistent knockdown of *Men-b* at the RNA level by qRT-PCR, using several different primer sets. Knockdown of lactate dehydrogenase (*Ldh*) was lethal to both wild-type and *tko*^{25t} larvae, making comparable experiments uninformative.

Despite their similar effects on eclosion timing (Figure 5), the addition of pyruvate and DCA to the low-sugar culture medium had opposite effects on the tissue levels of pyruvate and lactate in L3 larvae (Figure 8), although the changes were only significant for pyruvate levels (Tables S3). Pyruvate addition increased both lactate and pyruvate to levels comparable with those seen in high-sugar medium, whilst DCA lowered them, in accord with the expectation

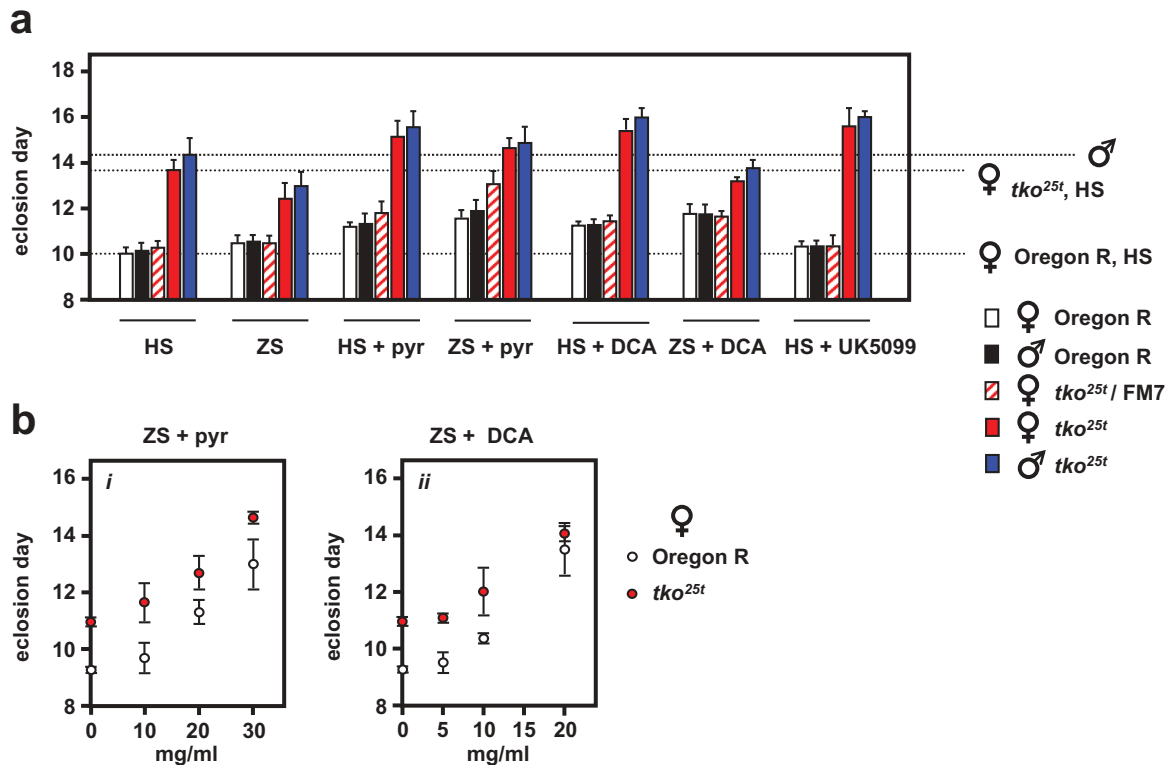


Figure 5. Drugs affecting pyruvate metabolism modify the *tko^{25t}* phenotype. Means \pm SD of times to eclosion of flies of the indicated genotypes and sex, at 25°C, on different media: HS – standard high-sugar medium, ZS – zero sugar medium, with addition of the indicated drugs that were present throughout the experiment: pyr – pyruvate, 25 mg/ml in (a) and concentrations as indicated in (b), DCA – dichloroacetate, 12.5 mg/ml in (a) and concentrations as indicated in (b), UK5099 – 25 μ g/ml. For statistical analysis of data from (a) by two-way ANOVA, see Figure S5. In summary, this revealed a significant effect of both genotype and drug addition ($p < 0.001$) for both diets and sexes, as well as an interaction between genotype and drug addition for both sexes on HS diet ($p < 0.01$) and for females only, on ZS diet ($p < 0.001$). Tukey *post hoc* HSD test ($p < 0.05$) was used, where appropriate, to determine the source of variation (see Figure S5 and comments in main text). Note that some of the data from (a) was previously published in [7], but without this statistical analysis, but is included here for full comparison. For a summary diagram of the reactions targeted by these drugs and by RNAi (see Figure 10).

that it would augment pyruvate metabolism by removing inhibition from (i.e. activating) PDH. The different effects of pyruvate and DCA imply that growth rate cannot be determined directly or solely by pyruvate concentration averaged across the tissues. Instead, a metabolite of pyruvate, or pyruvate in a specific intracellular or tissue-compartment, is likely to be instrumental.

Gene expression changes induced by pyruvate are non-coherent with those induced by *tko^{25t}*

Growth of *tko^{25t}* in high sugar was previously observed to downregulate some components of the protein synthetic and secretory machinery, as well as a number of key genes involved in developmental progression. These effects were seen also

seen in zero-sugar medium but were less pronounced. We used RNA-seq to test whether pyruvate addition produced the same changes in gene expression, applying similar criteria as in the previous study [7]. Using each of two parameters (i) absolute magnitude of changes measured by mass fraction (FPKM), and (ii) fold-change, we created lists of the genes showing the most pronounced alterations in expression due to pyruvate supplementation (Table S4). We considered both protein-coding and non-coding RNAs, as well as increases and decreases. From these ‘base-comparison’ lists of pyruvate-regulated genes (198 in the mass-fraction list and 248 in the fold-change list, applying arbitrary thresholds of >100 FPKM units or >eightfold change, Tables S4) we asked how many are regulated similarly in each of

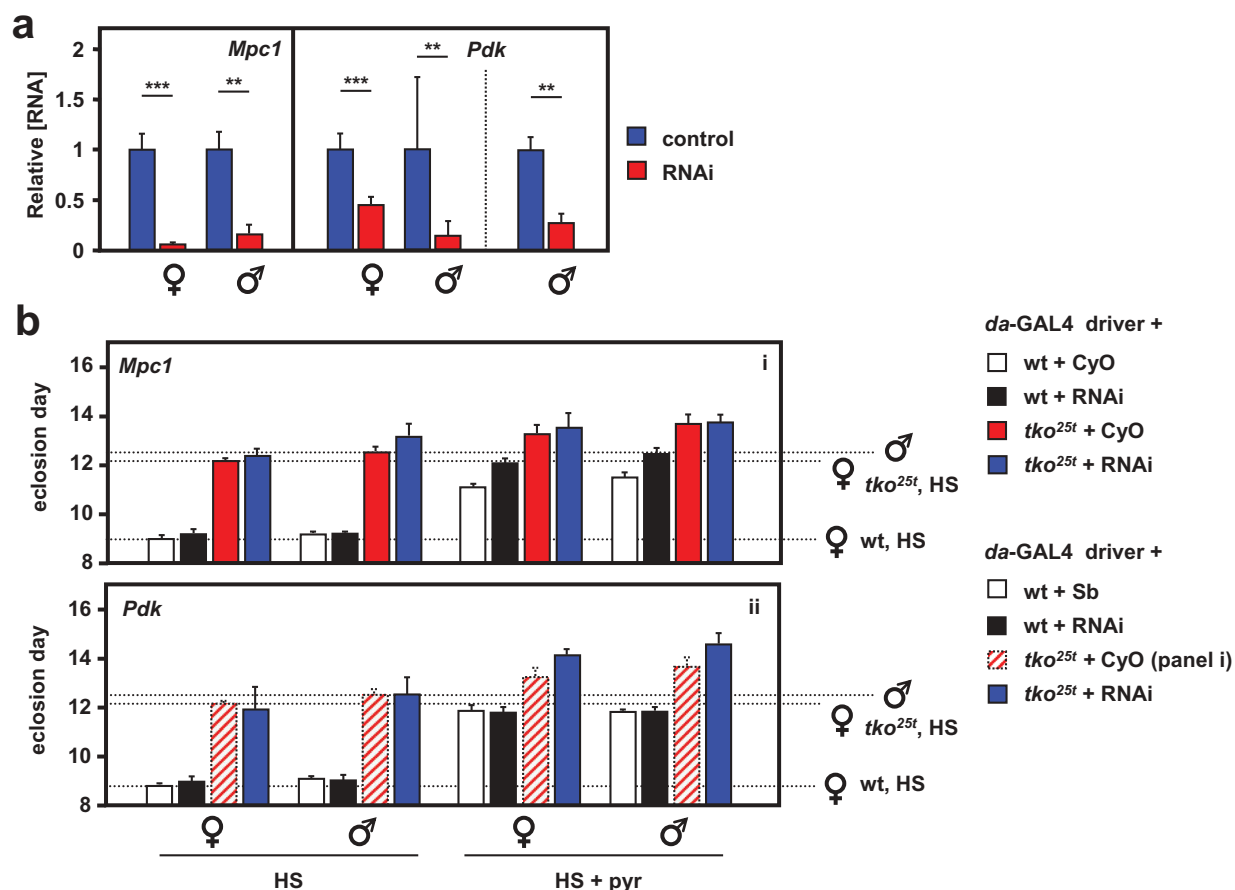


Figure 6. RNAi-mediated knockdown of *Mpc1* or *Pdk* modifies the *tko*^{25t} phenotype. (A) *Mpc1* or *Pdk* RNA levels measured by qRT-PCR and (B) time to eclosion of flies of the indicated genotypes (i.e. with relevant RNAi construct or balancer as shown), at 25°C, means ± SD, n ≥ 3 vials from each cross on the indicated medium: HS – high-sugar medium, with or without the addition of 25 mg/ml pyruvate. Horizontal dotted lines represent the mean eclosion times of Oregon R females and *tko*^{25t} females and males on HS medium, to facilitate comparisons. Statistical analysis by two-way ANOVA (Fig. S6) revealed a significant effect of genotype under all conditions, but both *Mpc1* and *Pdk* knockdown produced significant effects and showed significant interaction with genotype only in HS medium supplemented with pyruvate; *Mpc1* knockdown retarding the development only of wild-type and *Pdk* knockdown retarding only that of *tko*^{25t} flies of both sexes. Note that, in panel ii of (B), the CyO balancer flies from panel i, generated in the same experiment, are presented as the best indicative control. The TM3 balancer chromosome, whether marked with *Sb* or *Ser*, confers a developmental delay of >1 d that precludes its use as a control in such experiments, other than to allow identification of the non-balancer RNAi-bearing flies. Apart from this, all comparisons between control and knockdown flies of a given sex and genotype were from the same experiment, although Oregon R and *tko*^{25t} flies were analyzed from separate crosses, as were flies cultured on different media. For a summary diagram of the reactions targeted by RNAi and by various drugs see Figure 10.

six additional comparisons (Figure 9). In each output we considered the genes from the base-comparison list in five categories: those regulated in the same direction, either (i) above or (ii) below the arbitrary thresholds, those regulated in the opposite direction, again (iii) above or (iv) below threshold, and (v) those missing from the compared list, due to the initial statistical filtering. This analysis enabled us to draw the following conclusions, illustrated in Figure 9. First, most of the genes up- or down-regulated by pyruvate in wild-type larvae were regulated similarly by pyruvate

in *tko*^{25t} (comparison 1 in Figure 9). Second, only a minor subset of genes (≤15%) were regulated in the same direction by high-sugar (comparisons 2 and 3). Many genes were oppositely regulated by the presence of *tko*^{25t} (comparisons 4 and 5), and many pyruvate-regulated genes in wild-type showed either no effect or a change in the opposite direction in *tko*^{25t} larvae (comparison 6). The two approaches (mass-fraction and fold-change) gave similar outcomes. The functionally identified genes regulated similarly by pyruvate and by sugar were mostly linked to development

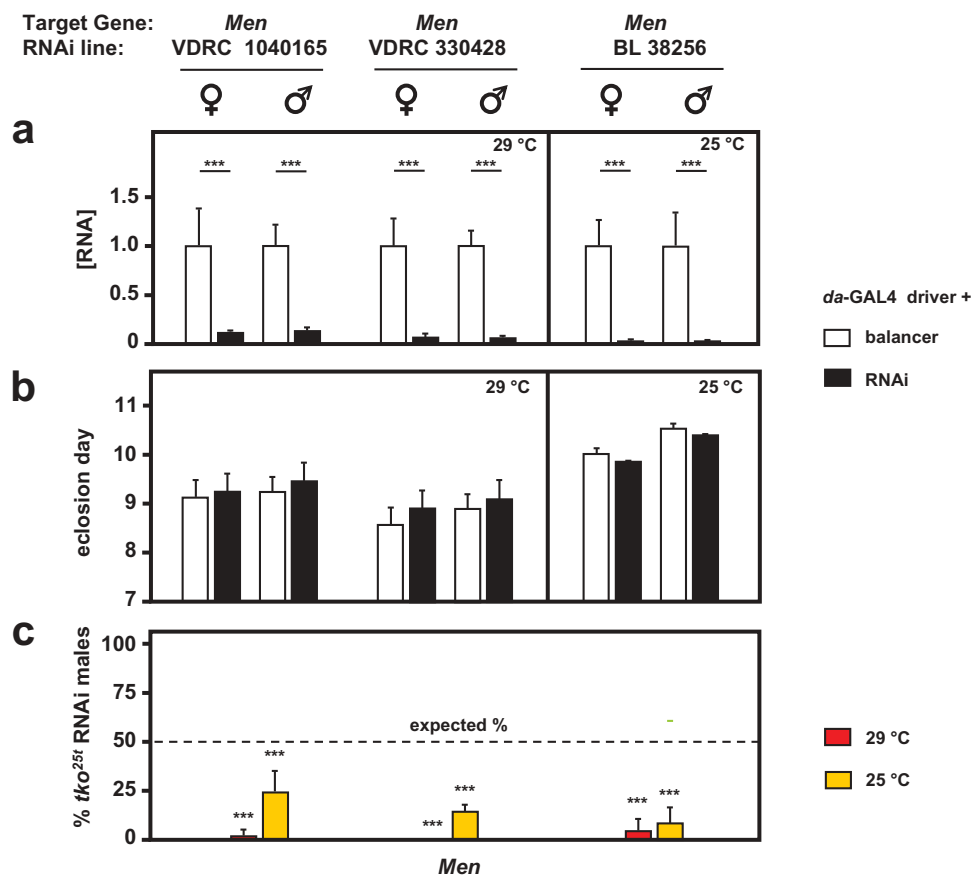


Figure 7. RNAi-mediated knockdown of *Men* (malic enzyme is synthetically (semi)lethal with *tko*^{25t}). (a) *Men* RNA levels measured by qRT-PCR and (b) time to eclosion of flies of the indicated genotypes (i.e. with relevant *Men* RNAi construct or balancer as shown), means \pm SD, $n \geq 3$ vials from each cross. Eclosion timing is shown for the temperature at which flies were also cultured for qRT-PCR (25°C or 29°C as shown). Eclosion timing at the other temperature was qualitatively similar, as shown in Fig. S4A. Horizontal bars denoted by asterisks (**) indicate significant differences, in pairwise comparisons of RNAi and balancer control flies of each given genotype and sex analyzed (Student's *t* test, $p < 0.001$). (c) Proportion (%) of eclosing RNAi male progeny that also carried *tko*^{25t}, as opposed to the FM7 balancer, from crosses of the general type: *tko*^{25t}/FM7; daGAL4 x FM7/Y; RNAi. Means \pm SD, $n \geq 3$ vials from each cross. Asterisks (***) above the bars denotes significant deviation from expected frequency of 50% (chi-squared test with Yates' continuity correction, $p < 0.001$). See also Fig. S4. For a summary diagram of the reactions targeted by RNAi and by various drugs see Figure 10.

(cuticular, muscle and a few gut proteins: Tables S5, sheet 1). Many of them, or others in the same functional categories, were oppositely altered in *tko*^{25t} (Tables S5, sheet 2). Many of the remaining genes regulated by dietary pyruvate, that were not affected by sugar or by *tko*^{25t}, code for components of the gene expression machinery or for OXPHOS and other mitochondrial functions (Table S4).

Discussion

Developmental delay in *tko*^{25t} depends on a systemic signal

Three lines of evidence presented in this paper support the idea that a systemic signal links

mitochondrial function to growth rate in *Drosophila* development. First, the developmental delay of *tko*^{25t} mutant larvae could be partially corrected (Figure 1) by expression of the wild-type allele via any of several different tissue-specific drivers, showing little or no overlap in the specificity of their expression (Fig. S1). Second, as far as could be demonstrated, these effects were additive (Figure 2, S4). Third, RNAi-mediated knockdown of *tko* using similarly specific drivers regenerated the mutant phenotype of *tko*^{25t}, including both developmental delay as well as (at least in some cases) bang-sensitivity. These observations imply that diminished mitochondrial function in a specific tissue is somehow integrated across the entire larva, presumably by

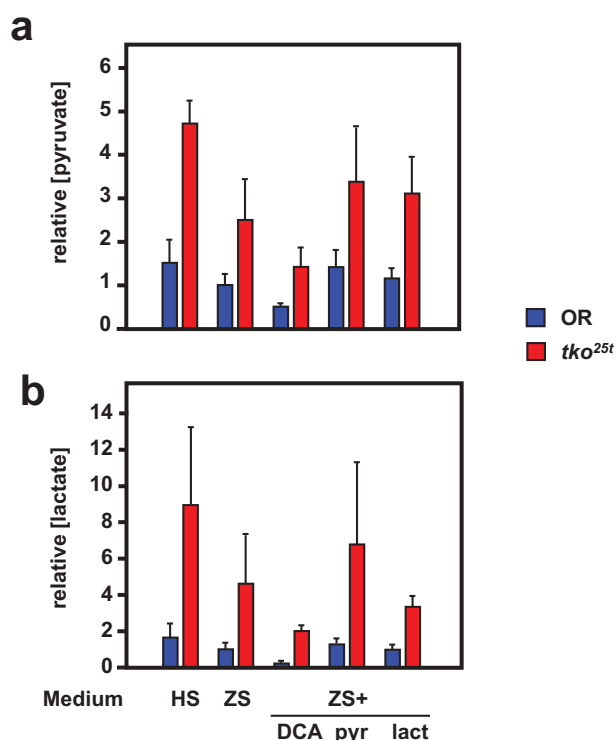


Figure 8. DCA modifies pyruvate and lactate levels oppositely from the effect of pyruvate addition. (a) Pyruvate and (b) lactate levels (means \pm SD, $n \geq 3$, generally four batches for each group) in L3 larvae of the indicated genotypes (OR = Oregon R wild-type). HS – high-sugar medium, ZS – zero-sugar medium, DCA – with addition of 12.5 mg/ml DCA, pyr, lact – with addition of 25 mg/ml pyruvate or lactate, respectively. Data are normalized to the values for wild-type on ZS medium. For statistical analysis, see Tables S3. For a summary diagram of the reactions targeted by drugs and RNAi see Figure 10.

the sharing of metabolites and their processing. Furthermore, this is not an all-or-none phenomenon, where growth is switched between two alternate programs whenever mitochondrial function crosses some threshold: the amount of developmental delay is variable, implying that the overall metabolic capacity of the larva is somehow being measured physiologically, and growth rate adjusted accordingly. These findings could be further strengthened by the use of additional drivers, especially in combination, although the problematic nature of the TM3 balancer means that we would need first to identify those carried on chromosome 3 that were viable as homozygotes (also with no maternal effects) and which had no unreported off-target expression patterns.

As indicated above, we hypothesized that such a signal could be either endocrine or metabolic in nature, or a combination of both. Endocrine signals

of metabolic – specifically mitochondrial stress are well established in other organisms, such as FGF21 or GDF15 in mammals [39]. Although both of these growth-factor superfamilies have representatives in insects, neither has a clear orthologue in *Drosophila*. The closest match to human GDF15, Glass bottom boat, is much more similar to other members of the BMP/TGF β superfamily, whilst none of the three *Drosophila* FGFs (Pyramus, Thisbe and Branchless) is a convincing match to human FGF21, and each of them plays a well-studied role in specific developmental programs (see [40] for review).

Two other well-known endocrine systems in *Drosophila* do provide a more direct connection between growth regulation and mitochondrial metabolism, namely the insulin-like peptides and the steroid hormone ecdysone. The insulin/IGF signalling system in the fly [41,42] is responsive to metabolic and nutritional signals to co-ordinate growth and behaviour, whilst ecdysteroids, partly synthesized in mitochondria [43,44], regulate progression between the different developmental stages, especially the onset of metamorphosis [45]. It will be worthwhile to study whether either interacts with *tko*^{25t}.

Tissue-specificity of the bang-sensitive phenotype

Bang-sensitivity is reported as a feature of mutants in two other genes for core functions of mitochondria, namely *sesB* (adenine nucleotide translocase) [46] and *kdn* (citrate synthase) [47]. These mutants, as well as *tko*^{25t}, show ATP depletion [47–49]. Global *tko* knockdown was here shown to phenocopy both the developmental delay (Figure 3) and bang-sensitivity (Figure 4) of the original *tko*^{25t} mutant, supporting the view that *tko*^{25t} is a simple hypomorph. However, the two phenotypes are clearly separable, based on the fact that the transgenic line UAS-*tko*⁺(8) shows no rescue of developmental delay in the absence of a GAL4 driver, but does exhibit effective rescue of bang-sensitivity [6], due, presumably, to an insertional effect [50]. The use of tissue-specific drivers to knock down *tko* sheds further light on this, since exclusively neuronal or muscle drivers both gave a bang-sensitive phenotype (Figure 4(a–c)), whereas a glial driver or one active in embryogenesis and in parts of the larval midgut (Fig. S1A) did not (Figure 4(d,e)). These findings imply

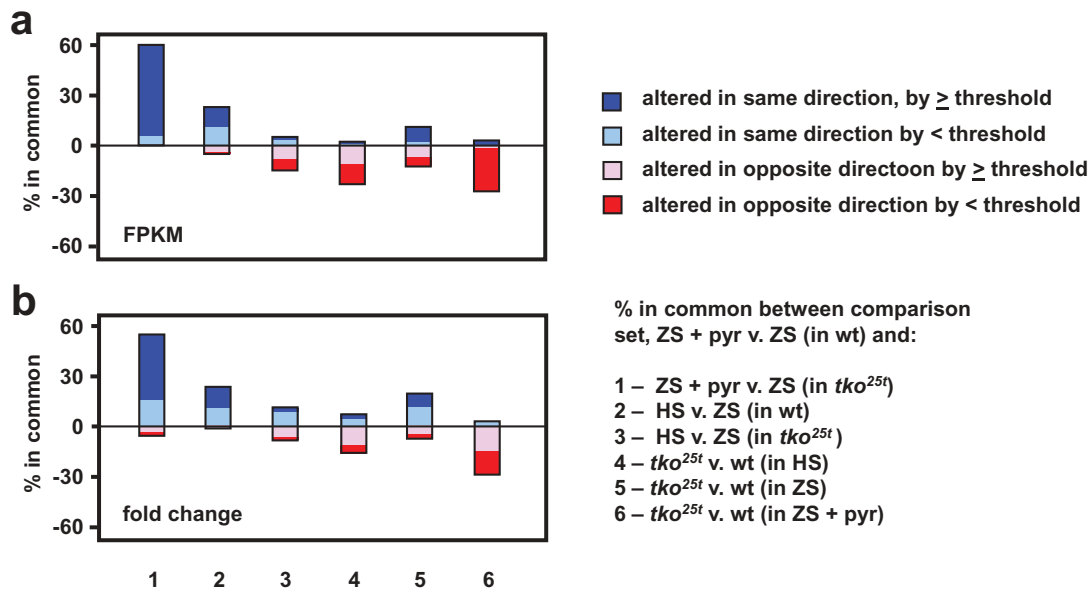


Figure 9. Gene expression changes induced by pyruvate are mostly different from those induced by high-sugar or *tko*^{25t}. Plotted comparisons are based on analysis by (a) FPKM (mass-fraction) and (b) fold-change, with arbitrary threshold of 100 FPKM units or eightfold change, respectively. The plot ignores the actual direction of change and the nature of the regulated transcripts (protein-coding or non-coding RNA) but instead shows whether the direction of change is the same or different between the base-comparison (genes regulated by pyruvate addition to zero-sugar medium) and the comparisons as enumerated. In each case, the changes to the remaining genes from the base-comparison set did not pass statistical filtering in the other comparisons.

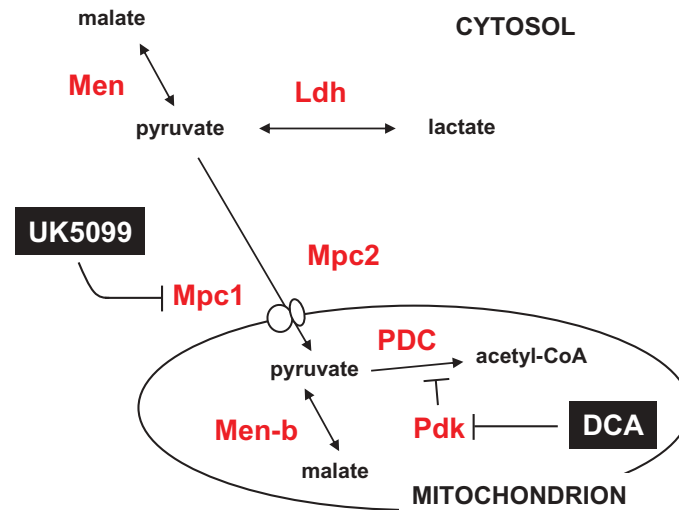


Figure 10. Summary diagram of steps in the pyruvate metabolic network targeted by drugs and RNAi. Metabolites are shown in black text, proteins in red, and drugs in white on black. Mpc1, Mpc2, Pdk, Men, Men-b and Ldh are shown by the systematic names from flybase. PDC – pyruvate dehydrogenase complex. For clarity, enzymes not targeted in the present experiments (such as pyruvate kinase and pyruvate carboxylase) are omitted.

that adequate mitochondrial OXPHOS capacity in muscle and in neurons, but not in other tissues, is required to avoid the prolonged paralytic seizures characteristic of *tko*^{25t}. The severity of the bang-sensitive phenotype produced by knockdown of *tko* using different GAL4 drivers is comparable with, or in some cases stronger, than that produced by *tko*^{25t}. However, since the relative strength of the various

tissue-specific drivers is not easily measured, the significance of this cannot be assessed.

***Lactate and pyruvate metabolism is linked to growth regulation in tko*^{25t}**

Candidates for a metabolic signal of mitochondrial dysfunction were already suggested by the previous

observation of elevated pyruvate and lactate levels in *tko*^{25t} larvae [7], and the fact that their addition to the culture medium phenocopied the effects of high-sugar on *tko*^{25t}. Serum lactate is already considered a key biomarker for diagnosing OXPHOS disorders in humans [39], whilst pyruvate has been identified as a crucial regulator of stemness and growth in mammalian cells [51]. In flies, the enzyme that interconverts lactate and pyruvate, lactate dehydrogenase (Ldh, or ImpL3) has previously been implicated as a target of growth signalling by the estrogen-related receptor [52]. This offered an attractive starting point for the present study.

Drugs and genetic manipulations that affect pyruvate metabolism (summarized in Figure 10) impacted the development of *tko*^{25t} (and, in some cases, wild-type flies), broadly supporting the view that pyruvate accumulation is a marker for a metabolic process that limits growth. The growth-inhibiting effects of pyruvate and of DCA were also dose-dependent. However, measurements of lactate and pyruvate levels in flies grown on different media (Figure 8) implied that neither was a direct predictor of developmental phenotype, which may instead depend on a downstream product of pyruvate metabolism. Thus, pyruvate or lactate supplementation resulted in only a modest increase in the steady-state level of pyruvate, whereas DCA, which substantially decreased pyruvate and lactate levels (Figure 8), produced paradoxical effects on developmental timing, accelerating the growth of *tko*^{25t} on zero-sugar medium, but retarding that of wild-type flies, whilst in high-sugar medium it compounded rather than alleviated *tko*^{25t} developmental delay (Figure 5(b)). Pdk knockdown exacerbated the developmental delay of *tko*^{25t} (Figure 6(b), ii), but only under conditions of pyruvate overload. Although DCA is a potent inhibitor of Pdk [53], it may also have other targets [54–56] and is accumulated in cells via the plasma-membrane monocarboxylate transporters, MCTs [57]. Moreover, in cancer cells, it has been reported to inhibit the pentose phosphate pathway [58] and thereby decrease the level of NADPH, which is already depleted in *tko*^{25t}, especially when grown on high-sugar medium [7]. Such off-target effects may account for the different outcomes of DCA treatment and *Pdk* knockdown.

UK5099, predicted to limit mitochondrial pyruvate utilization by inhibiting the mitochondrial

pyruvate carrier, produced a clear exacerbation of the *tko*^{25t} developmental phenotype (Figure 5(b)), whilst *Mpc1* knockdown produced different effects, slowing the growth of wild-type flies under pyruvate overload, but exhibiting only minor effects on *tko*^{25t} development that were essentially epistatic to the effect of added pyruvate (Figure 6(b), i). Although originally identified as an inhibitor of the mitochondrial pyruvate carrier [59], UK5099 was subsequently shown to block MCTs as well [60–63]. If it blocks lactate efflux *in vivo*, its net effect may be to increase cytosolic lactate and/or pyruvate independently of its effects on mitochondria, potentially accounting for the different outcome of *Mpc1* knockdown. Other, more specific inhibitors, such as PS10 for Pdk [64], or GW604714X and GW450863X for the mitochondrial pyruvate carrier [65], may prove useful in disentangling these effects, although their efficacy and specificity would need to be verified for *Drosophila*.

The findings with *Men* are also consistent with pyruvate being a critical metabolite, although the effect on *tko*^{25t} was lethality rather than extended development. One possibility is that a high level of pyruvate facilitates NADPH depletion via the NADPH-dependent conversion of pyruvate to malate catalyzed by *Men*. If, as hypothesized earlier, NADPH depletion is a critical element of growth signalling in *tko*^{25t} [7], a decreased capacity of pyruvate to malate conversion could undermine this signalling, with catastrophic consequences for a larva with severe limitations on TCA-cycle and biosynthetic flux, and ATP depletion.

Overall, whilst we can infer that manipulations affecting pyruvate and lactate metabolism affect growth-regulation in *tko*^{25t}, possible off-target or secondary effects of the drugs and knockdowns preclude a definitive mechanistic conclusion at this time. Unravelling the many possibilities will require the development of methods for assaying fluxes of the key metabolites at the subcellular level *in vivo*, considering separately the mitochondrial and cytosolic pools of pyruvate, malate, NADPH, ATP and their derivatives.

Pyruvate modulates growth rate translationally and/or post-translationally

Growth of *tko*^{25t} in high-sugar medium was previously observed to affect gene expression in two

ways: first, via a post-translational mechanism affecting S6K, second, via changes in transcript representation [7]. In the present study, we found that only a minor fraction of the genes regulated at the RNA level by pyruvate were regulated in the same way by high sugar, whilst those responding to *tko*^{25t} were mostly altered in the opposite direction. This was unexpected, given the fact that *tko*^{25t} responded similarly to pyruvate and high sugar, and suggests that global growth regulation in response to mitochondrial dysfunction and metabolic disturbance occurs mainly at the (post-)translational level. Regulation at the protein level is also suggested by the fact that the list of similarly or oppositely regulated genes at the RNA level includes very few that are connected either to metabolism or to transcription. It remains possible that relevant changes remain buried in the list of transcriptional targets because they change only by rather modest amounts that are below the thresholds set here but are nevertheless critical to the regulation of growth. More plausibly, a global regulator like the cyclin-dependent kinases or AMPK, which would not have to compete with cell-specific transcriptional programs, can respond to a systemic signal in broadly similar ways in all cells.

In conclusion, this study provides evidence that mitochondrial dysfunction triggers a systemic response that curtails the rate of growth of *Drosophila* larvae, and confirms a key role for pyruvate or its metabolic products in eliciting this signal.

Acknowledgments

We thank Shweta Manjiry, who conducted some preliminary experiments relevant to this paper, Eveliina Teeri and Essi Eräsalo for technical assistance, and Troy Faithfull for help with the manuscript.

Disclosure statement

No potential conflict of interest was reported by the authors. During the review process of the manuscript, corresponding author HTJ was appointed as Editor-in-Chief of the journal. However, he remained uninvolved in, and blinded to, the review and editorial process.

Funding

This work was supported by the Academy of Finland under Grants 283157 and 272376, the Tampere University Hospital Medical Research Fund and the Sigrid Juselius Foundation. The *Drosophila* work was carried out in the Tampere *Drosophila* Facility, partially funded by Biocenter Finland.

ORCID

Jack George  <http://orcid.org/0000-0002-0053-4171>

Tea Tuomela  <http://orcid.org/0000-0002-1010-0561>

Esko Kempainen  <http://orcid.org/0000-0002-5491-5391>

References

- [1] Thompson K, Collier JJ, Glasgow RIC, et al. Recent advances in understanding the molecular genetic basis of mitochondrial disease. *J Inherit Metab Dis*. 2019. [Epub before print]. DOI:10.1002/jimd.12104.
- [2] Kanungo S, Morton J, Neelakantan M, et al. Mitochondrial disorders. *Ann Transl Med*. 2018;6:475.
- [3] Murphy MP, Hartley RC. Mitochondria as a therapeutic target for common pathologies. *Nat Rev Drug Discov*. 2018;17:865–886.
- [4] Boczonadi V, Horvath R. Mitochondria: impaired mitochondrial translation in human disease. *Int J Biochem Cell Biol*. 2014;48:77–84.
- [5] Toivonen JM, O'Dell KM, Petit N, et al. *Technical knockout*, a *Drosophila* model of mitochondrial deafness. *Genetics*. 2001;159:241–254.
- [6] Toivonen JM, Manjiry S, Touraille S, et al. Gene dosage and selective expression modify phenotype in a *Drosophila* model of human mitochondrial disease. *Mitochondrion*. 2003;3:83–96.
- [7] Kempainen E, George J, Garipler G, et al. Mitochondrial dysfunction plus high-sugar diet provokes a metabolic crisis that inhibits growth. *PLoS One*. 2016;11:e0145836.
- [8] Wodarz A, Hinz U, Engelbert M, et al. Expression of *crumbs* confers apical character on plasma membrane domains of ectodermal epithelia of *Drosophila*. *Cell*. 1995;82:67–76.
- [9] Yin S, Qun Q, Zhou B. Functional studies of *Drosophila* zinc transporters reveal the mechanism for zinc excretion in Malpighian tubules. *BMC Biol*. 2017;15:12.
- [10] Osterwalder T, Yoon KS, White BH, et al. A conditional tissue-specific transgene expression system using inducible GAL4. *Proc National Acad Sci USA*. 2001;98:12596–12601.
- [11] Berger C, Renner S, Lürer K, et al. The commonly used marker ELAV is transiently expressed in neuroblasts and glial cells in the *Drosophila* embryonic CNS. *Dev Dyn*. 2007;236:3562–3568.

- [12] Sun B, Xu P, Wang W, et al. *In vivo* modification of Na⁺,K⁺-ATPase activity in *Drosophila*. *Comp Biochem Physiol B Biochem Mol Biol*. 2001;130:521–536.
- [13] Oland LA, Biebelhausen JP, Tolbert LP. The glial investment of the adult and developing antennal lobe of *Drosophila*. *J Comp Neurol*. 2008;509:526–550.
- [14] Górska-Andrzejak J, Salvaterra PM, Meinertzhagen IA, et al. Cyclical expression of Na⁺/K⁺-ATPase in the visual system of *Drosophila melanogaster*. *J Insect Physiol*. 2009;55:459–468.
- [15] Edwards TN, Meinertzhagen IA. The functional organisation of glia in the adult brain of *Drosophila* and other insects. *Prog Neurobiol*. 2010;90:471–490.
- [16] Stork T, Bernardos R, Freeman MR. Analysis of glial cell development and function in *Drosophila*. *Cold Spring Harb Protoc*. 2012;2012:1–17.
- [17] Wang J-W, Beck ES, McCabe BD. A modular toolset for recombination transgenesis and neurogenetic analysis of *Drosophila*. *PLoS One*. 2012;7:e42102.
- [18] Aberle H, Haghighi AP, Fetter RD, et al. *wishful thinking* encodes a BMP type II receptor that regulates synaptic growth in *Drosophila*. *Neuron*. 2002;33:545–558.
- [19] Kempainen KK, Rinne J, Sriram A, et al. Expression of alternative oxidase in *Drosophila* ameliorates diverse phenotypes due to cytochrome oxidase deficiency. *Hum Mol Genet*. 2014;23:2078–2093.
- [20] Ranganayakulu G, Elliott DA, Harvey RP, et al. Divergent roles for NK-2 class homeobox genes in cardiogenesis in flies and mice. *Development*. 1998;125:3037–3048.
- [21] Casso D, Ramírez-Weber FA, Kornberg TB. GFP-tagged balancer chromosomes for *Drosophila melanogaster*. *Mech Dev*. 1999;88:229–232.
- [22] Castelli-Gair JE, Greig S, Micklem G, et al. Dissecting the temporal requirements for homeotic gene function. *Development*. 1994;120:1983–1995.
- [23] Reiling JH, Hafen E. The hypoxia-induced paralogs Scylla and Charybdis inhibit growth by down-regulating S6K activity upstream of TSC in *Drosophila*. *Genes Dev*. 2004;18:2879–2892.
- [24] Takeuchi T, Suzuki M, Fujikake N, et al. Intercellular chaperone transmission via exosomes contributes to maintenance of protein homeostasis at the organismal level. *Proc National Acad Sci USA*. 2015;112:E2497–E2506.
- [25] Perkins LA, Holderbaum L, Tao R, et al. The transgenic RNAi project at harvard medical school: resources and validation. *Genetics*. 2015;201:843–852.
- [26] Yan D, Neumüller RA, Buckner M, et al. A regulatory network of *Drosophila* germline stem cell self-renewal. *Dev Cell*. 2014;28:459–473.
- [27] Pletcher RC, Hardman SL, Intagliata SF, et al. A genetic screen using the *Drosophila melanogaster* TRiP RNAi collection to identify metabolic enzymes required for eye development. *G3*. 2019;9:2061–2070.
- [28] Ni JQ, Zhou R, Czech B, et al. A genome-scale shRNA resource for transgenic RNAi in *Drosophila*. *Nat Methods*. 2011;8:405–407.
- [29] Dietzl G, Chen D, Schnorrer F, et al. A genome-wide transgenic RNAi library for conditional gene inactivation in *Drosophila*. *Nature*. 2007;448:151–156.
- [30] Judd BH, Shen MW, Kaufman TC. The anatomy and function of a segment of the X chromosome of *Drosophila melanogaster*. *Genetics*. 1972;71:139–156.
- [31] Royden CS, Pirrotta V, Jan LY. The *tko* locus, site of a behavioral mutation in *Drosophila melanogaster*, codes for a protein homologous to prokaryotic ribosomal protein S12. *Cell*. 1987;51:165–173.
- [32] Shah ZH, O'Dell KMC, Miller SCM, et al. Metazoan nuclear genes for mitoribosomal protein S12. *Gene*. 1997;204:55–62.
- [33] Merriam JR. FM7: a 'new' first chromosome balancer. *Drosophila Inf Serv*. 1969;44:101.
- [34] Lindsley DL, Zimm GG. The genome of *Drosophila melanogaster*. NY: Academic Press; 1992.
- [35] Barolo S, Carver LA, Posakony JW. GFP and beta-galactosidase transformation vectors for promoter/enhancer analysis in *Drosophila*. *BioTechniques*. 2000;29:726–732.
- [36] Lee T, Luo L. Mosaic analysis with a repressible neurotechnique cell marker for studies of gene function in neuronal morphogenesis. *Neuron*. 1999;22:451–461.
- [37] Fernandez-Ayala DJ, Sanz A, Vartiainen S, et al. Expression of the *Ciona intestinalis* alternative oxidase (AOX) in *Drosophila* complements defects in mitochondrial oxidative phosphorylation. *Cell Metab*. 2009;9:449–460.
- [38] Brand AH, Perrimon N. Targeted gene expression as a means of altering cell fates and generating dominant phenotypes. *Development*. 1993;118:401–415.
- [39] Finsterer J, Zarrouk-Mahjoub S. Biomarkers for detecting mitochondrial disorders. *J Clin Med*. 2018;7:16.
- [40] Muha V, Müller HA. Functions and mechanisms of fibroblast growth factor (FGF) signalling in *Drosophila melanogaster*. *Int J Mol Sci*. 2013;14:5920–5937.
- [41] Nässel DR, Liu Y, Luo J. Insulin/IGF signaling and its regulation in *Drosophila*. *Gen Comp Endocrinol*. 2015;221:255–266.
- [42] Grönke S, Clarke DF, Broughton S, et al. Molecular evolution and functional characterization of *Drosophila* insulin-like peptides. *PLoS Genet*. 2010;6:e1000857.
- [43] Gilbert LI. Halloween genes encode P450 enzymes that mediate steroid hormone biosynthesis in *Drosophila melanogaster*. *Mol Cell Endocrinol*. 2004;215:1–10.
- [44] Niwa R, Niwa YS. Enzymes for ecdysteroid biosynthesis: their biological functions in insects and beyond. *Biosci Biotechnol Biochem*. 2014;78:1283–1292.
- [45] Yamanaka N, Rewitz KF, O'Connor MB. Ecdysone control of developmental transitions: lessons from *Drosophila* research. *Annu Rev Entomol*. 2012;58:497–516.
- [46] Zhang YQ, Roote J, Brogna S, et al. *stress sensitive B* encodes an adenine nucleotide translocase in *Drosophila melanogaster*. *Genetics*. 1999;153:891–903.
- [47] Fergestad T, Bostwick B, Ganetzky B metabolic disruption in *Drosophila* bang-sensitive seizure mutants. *Genetics*. 2006;173:1357–1364.

- [48] Chen S, Oliveira MT, Sanz A, et al. A cytoplasmic suppressor of a nuclear mutation affecting mitochondrial functions in *Drosophila*. *Genetics*. 2012;192:483–493.
- [49] Vartiainen S, Chen S, George J, et al. Phenotypic rescue of a *Drosophila* model of mitochondrial ANT1 disease. *Dis Models Mech*. 2014;7:635–648.
- [50] Jacobs HT, Fernández-Ayala DJ, Manjiry S, et al. Mitochondrial disease in flies. *Biochim Biophys Acta*. 2004;1659:190–196.
- [51] Schell JC, Wisidagama DR, Bensard C, et al. Control of intestinal stem cell function and proliferation by mitochondrial pyruvate metabolism. *Nat Cell Biol*. 2017;19:1027–1036.
- [52] Tennessen JM, Baker KD, Lam G, et al. The *Drosophila* estrogen-related receptor directs a metabolic switch that supports developmental growth. *Cell Metab*. 2011;13:139–148.
- [53] Whitehouse S, Cooper RH, Randle PJ. Mechanism of activation of pyruvate dehydrogenase by dichloroacetate and other halogenated carboxylic acids. *Biochem J*. 1974;141:761–774.
- [54] Gong F, Peng X, Sang Y, et al. Dichloroacetate induces protective autophagy in LoVo cells: involvement of cathepsin D/thioredoxin-like protein 1 and Akt-mTOR-mediated signaling. *Cell Death Dis*. 2013;4:e913.
- [55] Woo SH, Seo SK, Park Y, et al. Dichloroacetate potentiates tamoxifen-induced cell death in breast cancer cells via downregulation of the epidermal growth factor receptor. *Oncotarget*. 2016;7:59809–59819.
- [56] Yang Y, Sun Y, Chen J, et al. AKT-independent activation of p38 MAP kinase promotes vascular calcification. *Redox Biol*. 2018;16:97–103.
- [57] Carpenter L, Halestrap AP. The kinetics, substrate and inhibitor specificity of the lactate transporter of Ehrlich-Lette tumour cells studied with the intracellular pH indicator BCECF. *Biochem J*. 1994;304:751–760.
- [58] De Preter G, Neveu MA, Danhier P, et al. Inhibition of the pentose phosphate pathway by dichloroacetate unravels a missing link between aerobic glycolysis and cancer cell proliferation. *Oncotarget*. 2015;7:2910–2920.
- [59] Halestrap AP. The mitochondrial pyruvate carrier: kinetics and specificity for substrates and inhibitors. *Biochem J*. 1975;148:85–96.
- [60] Wiemer EA, Michels PA, Opperdoes FR. The inhibition of pyruvate transport across the plasma membrane of the bloodstream form of *Trypanosoma brucei* and its metabolic implications. *Biochem J*. 1995;312:479–484.
- [61] Halestrap AP, Price NT. The proton-linked monocarboxylate transporter (MCT) family: structure, function and regulation. *Biochem J*. 1999;343:281–299.
- [62] Yang J, Ruchti E, Petit JM, et al. Lactate promotes plasticity gene expression by potentiating NMDA signaling in neurons. *Proc National Acad Sci USA*. 2014;111:12228–12233.
- [63] Baufeld A, Vanselow J. Lactate promotes specific differentiation in bovine granulosa cells depending on lactate uptake thus mimicking an early post-LH stage. *Reprod Biol Endocrinol*. 2018;16:15.
- [64] Wu CY, Satapati S, Gui W, et al. A novel inhibitor of pyruvate dehydrogenase kinase stimulates myocardial carbohydrate oxidation in diet-induced obesity. *J Biol Chem*. 2018;293:9604–9613.
- [65] Hildyard JC, Ammälä C, Dukes ID, et al. Identification and characterisation of a new class of highly specific and potent inhibitors of the mitochondrial pyruvate carrier. *Biochim Biophys Acta*. 2005;1707:221–230.